THE ASTRONOMICAL JOURNAL, 119:478–485, 2000 February
© 2000. The American Astronomical Society. All rights reserved. Printed in U.S.A.

ASCA OBSERVATIONS OF THE GIGAHERTZ-PEAKED SPECTRUM RADIO GALAXIES 1345+125 AND 2352+495

CHRISTOPHER P. O'DEA
Space Telescope Science Institute,[1] 3700 San Martin Drive, Baltimore, Maryland 21218; odea@stsci.edu
WILLEM H. DE VRIES[2]
Space Telescope Science Institute, 3700 San Martin Drive, Baltimore, Maryland 21218; devries@stsci.edu
D. M. WORRALL
Department of Physics, University of Bristol, Tyndall Avenue, Bristol Bs8 1TL, England, UK; D.Worrall@Bristol.ac.uk
STEFI A. BAUM
Space Telescope Science Institute, 3700 San Martin Drive, Baltimore, Maryland 21218; sbaum@stsci.edu
AND
ANTON KOEKEMOER
Space Telescope Science Institute, 3700 San Martin Drive, Baltimore, Maryland 21218; koekemoe@stsci.edu
Received 1999 July 29; accepted 1999 October 25

ABSTRACT

We present *ASCA* SIS and GIS observations of two GHz peaked spectrum (GPS) radio galaxies, PKS 1345+125 (4C12.50, $z = 0.122$) and 2352+495 ($z = 0.237$). In the energy band 2–10 keV, 1345+125 is detected with about 2×10^{43} ergs s^{-1}, while 2352+495 is not detected with an upper limit $< 7 \times 10^{42}$ ergs s^{-1}. This is the first reported detection of X-ray emission from a GPS radio galaxy. These measurements do not violate predictions of Heinz et al.'s recent evolving source model for radio sources, although deeper X-ray observations are needed for a strong test of the model. The host galaxy of 1345+125 contains two nuclei separated by 2″ (4 kpc) which are not resolved by the *ASCA* observations. We suggest that the X-rays are emitted by the western of the two nuclei, which Gilmore & Shaw have shown has a NLRG/Seyfert-2 optical spectrum and which Evans et al. have recently identified with the GPS radio source. We obtain model dependent estimates for the 1345+125 radio source age of about 3×10^4 yr and expansion velocity of approximately 0.02*c*. We show that in samples of Seyfert 1's and powerful *extended* radio galaxies, optical emission-line luminosities are of a strength consistent with photoionization by the embedded active galactic nucleus (AGN; estimated using *ASCA* observations), and 1345+125 fits this picture assuming the X-ray emission is from the western nucleus. In contrast, the extrapolated limits on the nuclear ionizing continuum in 2352+495 are too low to account for the luminosity of the narrow emission-line region. If this is confirmed by further observations, it would favor a model in which some fraction of the emission lines are powered by shocks induced by the radio source or in which some of the AGN photons that ionize the gas are obscured from our view.

Key words: galaxies: active — galaxies: elliptical and lenticular, cD — galaxies: nuclei — galaxies: Seyfert — X-rays

1. INTRODUCTION

Recent work has identified the GHz peaked spectrum (GPS) and compact steep spectrum (CSS) radio sources as the most likely candidates for the progenitors of the large-scale powerful radio sources (e.g., Fanti et al. 1995; Readhead et al. 1996a, 1996b; O'Dea & Baum 1997). The GPS and CSS sources are powerful but compact radio sources whose spectra are generally simple and convex with peaks near 1 GHz and 100 MHz respectively (O'Dea, Baum, & Stanghellini 1991; Fanti et al. 1990; for a review see O'Dea 1998). The GPS sources are entirely contained within the extent of the narrow-line region ($\lesssim$1 kpc), while the CSS sources are contained entirely within the host galaxy ($\lesssim$15 kpc). Current models for the evolution of powerful radio galaxies suggest that these sources propagate from the approximately 100 pc to megaparsec scales at roughly constant velocity through an ambient medium that declines in density as $\rho(R) \propto R^{-2}$, while the sources decline in radio luminosity as $L_{\rm rad} \propto R^{-0.5}$ (Fanti et al. 1995; Begelman 1996; O'Dea & Baum 1997; Readhead et al. 1996a; De Young 1997; cf. Carvalho 1985; Snellen et al. 1998). X-ray observations probe the interstellar medium (ISM) of the host galaxy and provide constraints on the evolution of the radio sources.

In our previous ROSAT PSPC observations of the GPS radio galaxies PKS 1345+125 and 2352+495, these sources were not detected (O'Dea et al. 1996b; hereafter Paper I), providing constraints on the AGN luminosity and environments of these sources. We obtained deeper observations with the hard energy sensitivity of *ASCA* in order to determine whether the lack of detection of the AGN in soft X-rays was due to the sources being intrinsically weak or to the presence of large absorbing columns.

We adopt $H_0 = 75$ km s^{-1} Mpc^{-1} and $q_0 = 0.1$ for consistency with Paper I.

2. DATA REDUCTION AND ANALYSIS

The properties of the sources are given in Table 1. The source 1345+125 was observed with *ASCA* on 1996 July 20 for a total of 19 ks, whereas 2352+495 was observed on

[1] Operated by the Association of Universities for Research in Astronomy, Inc. under cooperative agreement with the National Aeronautics and Space Administration.
[2] Also at Kapteyn Astronomical Institute, University of Groningen.

TABLE 1

SOURCE LIST

PARAMETER	SOURCE	
	1345+125	2352+495
z	0.122	0.237
$m(R_c)$	15.2	17.8
$M(R_c)$	−23.5	−22.6
$D_{\rm lum}$ (Mpc)	514	1050
Scale (kpc arcsec^{-1})	2.0	3.3
R.A. (J2000.0)	$13^h47^m33^s.36$	$23^h55^m09^s.46$
Decl. (J2000.0)	12°17′24″.2	49°50′08″.2
log $P_{1.4}$ (Watts Hz^{-1})	26.21	26.54
Linear size (kpc)	0.25	0.50
Galactic column (cm^{-2})	1.1×10^{20}	1.2×10^{21}
Hα flux (ergs s^{-1} cm^{-2})	$<2 \times 10^{-15}$ (nonactive) 2.0×10^{-14} (active)	7.8×10^{-16}

NOTE.—A summary of global source properties. The references for the redshifts are Gilmore & Shaw (1986), 1345+125; Lawrence et al. (1996), 2352+495. The Cousins R_c apparent and absolute magnitude for 1345+125 and 2352+495 are taken from O'Dea et al. (1996a). We adopt $H_0 = 75$ km s^{-1} Mpc^{-1} and $q_0 = 0.1$. The Galactic H I column densities are from Lockman (1991, private communication) and have 5% uncertainties. References for Hα fluxes are: 1345+125, Baum et al. (1988) and Axon et al. (1999); 2352+495, Lawrence et al. (1996).

1996 August 2 for 18 ks. In both observations, both the gas-filled imaging spectrometers (GIS2 and GIS3) operated in pulse height (PH) mode, with MEDIUM and HIGH telemetry rates. The solid state imaging spectrometers (SIS0 and SIS1) operated in the 1 CCD FAINT mode, with the data on the ground converted to BRIGHT mode (see *ASCA* Data Reduction Guide 1998[3]). A log of the observations can be found in Table 2, and Table 3 gives the net count rates.

TABLE 2

ASCA X-RAY OBSERVATIONS

Name	Sequence	Date	Exposure (s)	Instrument
1345+125.....	74067000	1996 Jul 20	19562	GIS2/3
			19622	SIS0
			19338	SIS1
2352+495.....	74068000	1996 Aug 2	18366	GIS2/3
			18184	SIS0
			19119	SIS1

TABLE 3

ASCA NET COUNT RATES

Name	SIS0	SIS1	GIS2	GIS3
1345+125.....	11.0 ± 1.2	8.3 ± 1.2	6.4 ± 1.1	10.9 ± 1.2
2352+495.....	<1	<1	<1	<1

NOTE.—These are net (background subtracted) count rates in the 4 different *ASCA* detectors. Units are counts ks^{-1}. Upper limits are 3 σ.

The analysis was performed on the data with the standard GSFC screening criteria applied. For the SIS analysis only grades 0, 2, 3, and 4 were used. The LOW telemetry mode data for the GIS detectors in the case of 1345+125 were discarded (only a few minutes effectively on source). The FTOOLS (version 3.6) task XSELECT was used to apply the necessary spatial filters. For the GIS instruments, we used a circular aperture with an approximately 4′.3 radius, in the SIS cases this radius was reduced to approximately 2′.6. This aperture was centered on the source or, in the case of 2352+495, where nothing obvious could be seen, at the expected source position. The background data were extracted from nearby clean patches of sky from the on-source exposures. Comparison of the locally derived background with that extracted from archival deep background images showed no significant differences.

1345+125 (Fig. 1) was detected in the combined GIS and combined SIS images. However, 2352+495 was not detected in either the GIS or SIS images.

2.1. *Spectral Analysis*

We have combined the extracted GIS spectra for 1345+125, where there is a detection (Fig. 2). All the sub-

[3] Available at http://asca.gsfc.nasa.gov/docs/asca/abc/abc.html.

TABLE 4

SPECTRAL FIT TO 1345+125

$n_{\rm H}$	Γ	Norm
$4.2(+4.0,-2.4) \times 10^{22}$ cm^{-2}.....	$1.6(+1.2,-0.8)$	$2.4(+16.6,-1.9) \times 10^{-4}$

NOTE.—These are the best fitting parameters to an absorbed power-law model which includes the known Galactic foreground absorbing column. Errors are 67% confidence limits for two interesting parameters based on a $\delta\chi^2 = 1$.

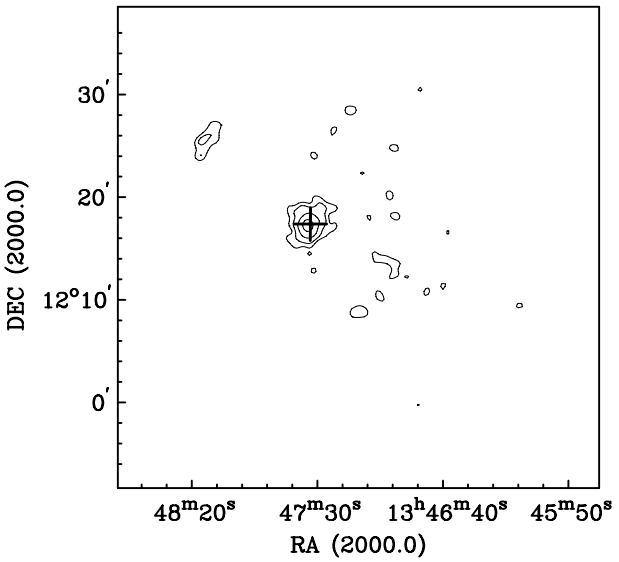


FIG. 1.—1345+125. GIS2+3 combined image with a lowest contour of 3 σ above the sky. Image has been smoothed with a Gaussian of FWHM 1′ (comparable to the instrumental PSF). The source is unresolved. The cross marks the location of the GPS source.

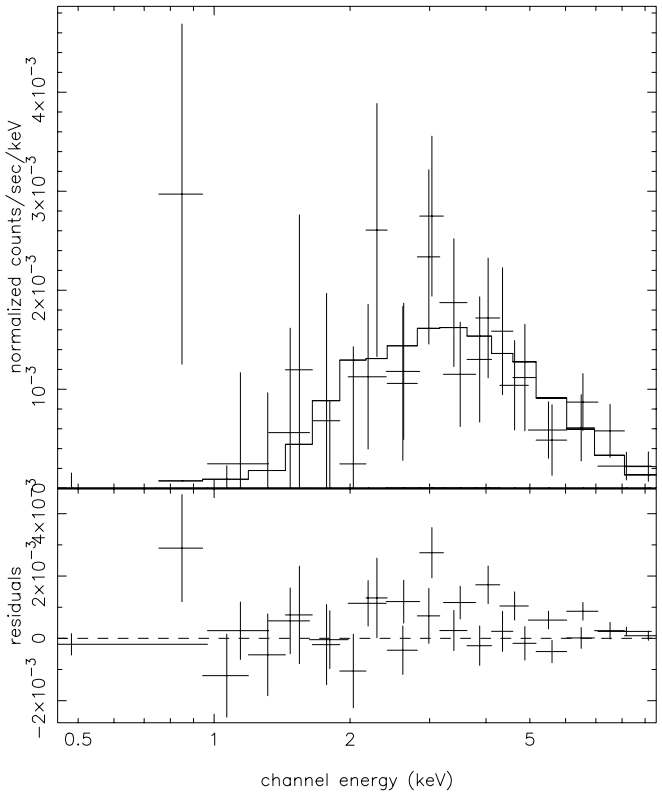


FIG. 2.—1345+125. GIS 2 and 3 spectra (*crosses*) with best-fit model superposed (where the model is fit to the combined spectrum; Table 4) with an intrinsic column density of 4×10^{22} cm^{-2} and a photon index of $\Gamma = 1.6$. The spectrum is regrouped to ensure at least 30 counts bin^{-1}. Note that the error bars in the plot are symmetric but are truncated at the lower edge of the plot.

sequent analysis was done with FTOOLS XSPEC, version 10. With the XSPEC task GRPPHA the spectra were regrouped into bins with a minimum of 30 counts per bin in order for the errors to be considered Gaussian. We fitted an absorbed power-law model to the data (intrinsic absorption plus fixed Galactic column), and results are found in Figure 2 and Tables 4 and 5. The higher redshift source 2352+495 was not detected even when all bins were combined.

3. IMPLICATIONS FOR GPS RADIO GALAXIES

Our ROSAT PSPC observations showed that the GPS radio galaxies are weak in *soft* X-rays, with luminosities in the 0.2–2 keV Band of $L_x \lesssim 3 \times 10^{42}$ ergs s^{-1}, Paper I. These observations constrained the environments of the sources to be poor clusters or groups and ruled out the presence of cooling flows larger than a few solar masses per year. The pressure in any hot ISM in the host galaxies is too low to confine the radio sources and (unless they are confined by warm or cold gas) they must be expanding in ram pressure balance with the external medium. The nondetection of the GPS nuclei by ROSAT could be due to either an intrinsically weak AGN or to high column densities. We noted that columns of 10^{22} cm^{-2} and higher could successfully hide AGN luminosities of a few times 10^{43} ergs s^{-1} in the 0.2–2 keV band.

Our new *ASCA* observations are consistent with our ROSAT results. In the energy band 2–10 keV, 1345+125 is detected at a level of about 2×10^{43} ergs s^{-1}, while 2352+495 is not detected at a level of less than 7×10^{42} ergs s^{-1}.

3.1. *Constraints on the AGN*

It is interesting to compare our results with those of Seyfert galaxies, the class of AGN that is currently best studied with *ASCA*. At soft X-rays Seyfert 2's are orders of magnitude fainter than Seyfert 1's (e.g., Kriss, Canizares, & Ricker 1980). However, when observed with the hard X-ray sensitivity of *ASCA*, Seyfert 2's are found to have 2–10 keV X-ray luminosities which significantly overlap those in Seyfert 1's (L_x(Sy2) $\sim 10^{41-44}$ and L_x(Sy1) $\sim 10^{42-45}$ ergs s^{-1}), and to have large column densities of atomic hydrogen

TABLE 5

X-RAY FLUXES AND LUMINOSITIES

Name	Flux Density at 2 keV (μJy)	Flux 2−10 keV (10^{-13} ergs cm^{-2} s^{-1})	Luminosity 2−10 keV (10^{43} ergs s^{-1})
1345+125.....	0.06	9.0	2.2
2352+495.....	<0.002	<0.6	<0.7

NOTE.—The higher signal-to-noise GIS 2+3 results are presented here. The SIS0 and SIS1 data give consistent results. Upper limits are 3 σ. The derived flux and intrinsic luminosity are model dependent and assume that the spectrum is an absorbed power law. The best-fit model for 1345+125 given in Table 4 was also adopted for 2352+495.

$N(\mathrm{H}) \sim 10^{21-24}$ cm^{-2} toward their nuclei (e.g., Turner et al. 1997, 1998; Nandra et al. 1997; Reynolds 1997).

3.1.1. *1345+125*

The host galaxy of PKS 1345+125 contains two nuclei a mere 2″ (4 kpc) apart, indicating an ongoing merger (Gilmore & Shaw 1986; Heckman et al. 1986; Hutchings 1987; Sanders et al. 1988; Baum et al. 1988; Stanghellini et al. 1993; Surace et al. 1998; Evans et al. 1999). The southeast nucleus is optically dull while the northwest nucleus has a narrow-line radio galaxy/Seyfert-2–type optical spectrum (Grandi 1977; Gilmore & Shaw 1986; Baum, Heckman, & van Breugel 1992; Gelderman & Whittle 1994; Kim, Veilleux, & Sanders 1998). Since these two nuclei are not resolved by the *ASCA* observations, the interpretation of the results depends on which of the two nuclei is associated with the X-ray and radio source. The original astrometry by Gilmore & Shaw (1986) suggested that the eastern (optically dull) nucleus was associated with the GPS radio source. In this case, since the X-ray luminosity is similar to those of Seyfert galaxies, it would be uncertain whether the observed X-rays were emitted by the GPS radio nucleus or the emission-line (radio-quiet) nucleus. More recent astrometry (Stanghellini et al. 1993; Evans et al. 1999) suggests that the western (emission-line) nucleus is in fact associated with the GPS radio source. This would be more consistent with a picture in which the X-ray emission is also emitted by the western nucleus. In the following discussion we assume that this is the correct identification.

We note that the western nucleus appears to be quite gas rich. The presence of substantial amounts of gas in this system is supported by several pieces of evidence. (1) 1345+125 is an ultra luminous infrared galaxy (e.g., Golombek, Miley, & Neugebauer 1988). (2) $^{12}\mathrm{CO}(1 \rightarrow 0)$ is detected in emission (Mirabel, Sanders, & Kazes 1989; Evans et al. 1999) with an estimated mass of molecular hydrogen of order $M(\mathrm{H}_2) \sim 3.3 \times 10^{10}\ M_\odot$ (assuming the conversion derived for Galactic molecular clouds, e.g., Bloemen et al. 1986; Scoville & Sanders 1987; Young & Scoville 1991). Evans et al. (1999) detect the same CO luminosity in their 2.2″ FWHM OVRO beam as do Mirabel et al. in their 81″ FWHM NRAO 12 m beam, showing that the molecular gas is concentrated to within approximately the inner 2 kpc of the galaxy. The average number density of molecular hydrogen is $n(\mathrm{H}_2) \gtrsim 40$ cm^{-3} and the average column density of molecular hydrogen is $N(\mathrm{H}_2) \gtrsim 2 \times 10^{23}$ cm^{-2}. The CO derived average column density is comparable to though somewhat larger than the column density estimated from the X-ray observations (Table 4), possibly because the molecular gas is patchy or the CO/H_2 conversion factor is different in 1345+125. (3) H I absorption is detected against the radio source (Mirabel 1989). Assuming a uniform covering factor of the H I over the radio source, the H I column density is $N(\mathrm{H}) \simeq 6.2 \times 10^{18} T_s$ cm^{-2} where T_s is the spin temperature (Mirabel 1989). For values of spin Temperature of 100–1000 K the column density of atomic hydrogen is $N(\mathrm{H}) \sim 6 \times 10^{20-21}$ cm^{-2}.

Although the western nucleus has an optical spectrum characterized by narrow lines, in the near-IR broad Paα (FWHM $\sim$2600 km s^{-1}) is seen (Veilleux, Sanders, & Kim 1997; Perlman 1997, private communication). Hurt et al. (1999) report *HST*/FOC ultraviolet observations that show extended polarized UV continuum light[4] with the E-vector approximately perpendicular to the radio source axis. Both the UV polarization and the broad Paα indicate that 1345+125 has a hidden (but not too deeply hidden) quasar.

In the context of some simple assumptions, we can use the sizes of the emission-line nebula and radio source to obtain crude constraints on the age and expansion velocity of the radio source. We assume that the AGN became active simultaneously in the radio and optical, i.e., the emission-line nebula and the radio source are roughly the same age. We also assume the emission-line nebula is photon-bounded (with the ionizing photons originating either from the AGN or shocks around the radio source), and thus that the size of the nebula will grow with time. When the AGN turns on, the ionizing photons will start to propagate outward into the ISM with a velocity that depends on the conditions in the ISM. If the nebula is composed of clouds with a low filling factor imbedded in a hot ($T \sim 10^6$ K) intercloud medium, the ionizing photons travel mostly through the hot gas and the size of the nebula expands near the speed of light. When the clouds have a high filling factor (e.g., >0.1) then the speed of the ionization front is dominated by its propagation into the warm ($T \lesssim 10^4$ K) and/or neutral gas. In the case of an ionization front powered by radio source shocks of order half the optical line widths ($\sim$1500 km s^{-1}), the estimated ionization front speed ranges up to several thousand km s^{-1} (depending primarily on the shock velocity, Dopita & Sutherland 1996). Likewise, for the estimated ionizing luminosity from the AGN (Table 7) the speed of the ionization front into warm, ionized/neutral gas is of order several hundred to several thousand km s^{-1} (depending on the range of density). If the nebula extent expands at these speeds this would imply a very old age for the nebula and radio source ($\gtrsim 10^6$ yr), which would in turn imply very low expansion velocity for the radio source ($\lesssim$100 km s^{-1}) that is too low to drive shocks at the speed implied by the observed line widths. Thus, ionization front speeds of order $<10^4$ km s^{-1} are inconsistent with the expectation that the optical line widths are driven by interaction with the radio source (at least on the hundred pc scale), however, we cannot rule it out at this point.

Thus, the ratio of the sizes of the radio source and the nebula constrains the time-averaged expansion velocity of the radio source. The emission-line nebula is about 4.″4 (8.8 kpc) in radius (Baum et al. 1988) corresponding to an age of $\sim 3 \times 10^4 (v_{\mathrm{neb}}/c)^{-1}$ yr where v_{neb} is the actual expansion speed of the nebula. The projected length of the radio source from the likely core to the end of the southern radio lobe is 80 mas (160 pc) (Stanghellini et al. 1997). This gives an average expansion velocity of $0.018c(v_{\mathrm{neb}}/c)$. This velocity is an order of magnitude slower than that found in a few Compact Symmetric Sources so far (Owsianik & Conway 1998; Conway 2000). The slower expansion we estimate in 1345+125 is consistent with the relaxed appearance of the southern radio lobe and the existence of high gas densities in the nucleus.

3.1.2. *2352+495*

2352+495 is the archetype for the class of compact symmetric sources (Readhead et al. 1996b). Figure 3 shows the

[4] Curiously, the Hurt et al. position measured on the FOC image suggests that the *eastern* nucleus is the source of the UV light. This would be relatively large but not impossible for a *HST* Guide Star error.

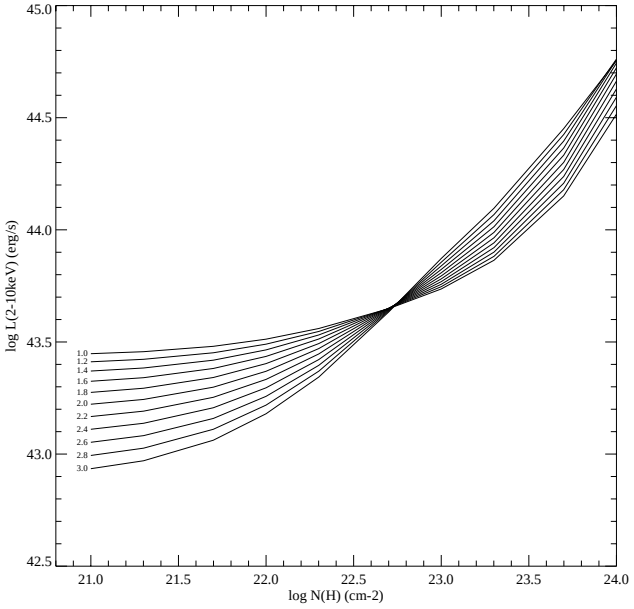


FIG. 3.—Possible intrinsic luminosity of 2352+495, which would remain undetected in our *ASCA* observations for different values of absorbing column for a range of power law Γ (such that $N(E)dE \propto E^{-\Gamma}dE$, where $N(E)$ is the photon flux density at energy E) and using the observed Galactic H I column.

possible intrinsic luminosity that would remain undetected in our *ASCA* observations for different values of absorbing column, and power-law photon index, and adopting the observed Galactic H I column (values of intrinsic energy adopting $\Gamma = 2$ are tabulated in Table 6). We find that a column of a few times 10^{23} cm^{-2} or greater could hide a luminosity of 10^{44} ergs s^{-1}. Thus, our limit on the X-ray luminosity of 2352+495 suggests that either the AGN is weaker than typical Seyfert galaxies and all currently detected quasars and broad line radio galaxies (but still consistent with low luminosity Seyferts) or the absorbing columns are higher than those in typical Seyferts and all currently detected quasars and BLRGs[5] (e.g., Reynolds 1997; Reeves et al. 1997; Sambruna et al. 1998 Allen et al. 1997; Brunetti et al. 1999, Woźniak et al. 1998). We note that there is currently no evidence for columns that large. The detection of H I absorption against the radio nucleus is consistent with columns of order 10^{22} cm^{-2} (G. Taylor 1998, private communication). However, Gallimore et al. (1999) have found no correlation between column densities derived from H I absorption in the 21 cm line and X-ray absorption in Seyferts. Gallimore et al. suggest that the radio and X-ray measurements are probing different paths through the nuclei possibly because the radio probes larger scales than the X-ray emission. Readhead et al. (1996b) report an upper limit of 0.1 for the optical depth in the ^{12}CO 1–0 line. However, this is difficult to interpret directly in terms of an absorbing column because the nonthermal radio continuum may increase the CO excitation temperature, thus reducing the observed optical depth (Maloney, Begelman, & Rees 1994).

TABLE 6

CONSTRAINTS ON OBSCURED NUCLEAR X-RAY LUMINOSITY IN 2352+495

$N_{H_{Intrinsic}}$ (cm^{-2})	Maximum Luminosity ($\times 10^{43}$ ergs s^{-1})
1×10^{21}.....	1.7
2×10^{21}.....	1.8
5×10^{21}.....	2.0
1×10^{22}.....	2.3
2×10^{22}.....	3.0
5×10^{22}.....	4.4
1×10^{23}.....	6.2
2×10^{23}.....	9.2
5×10^{23}.....	20
1×10^{24}.....	50

NOTE.—Upper limits to intrinsic 2–10 keV luminosity as a function of obscuring column, which would be consistent with our *ASCA* observations. We adopt a power-law photon index of $\Gamma = 2.0$ and include the measured Galactic column density $N(\mathrm{H}) \simeq 1.2 \times 10^{21}$ cm^{-2}. These luminosity constraints are calculated without binning the spectra, thus yielding less sensitive results than Table 5 for the specific "best-fit" value of N_{H}, but yielding more robust results for higher and lower values of absorbing column since all the spectral information is retained.

3.2. *Constraints on the Evolving Source Model*

Heinz, Reynolds, & Begelman (1998) have presented a model for the expected X-ray emission from a young, evolving radio galaxy as it propagates through its host galaxy ISM or the ICM. In this model, the X-ray emission is produced in the surrounding shell of gas, which is shocked by the expansion of the radio lobe. C. Reynolds has kindly provided a program which we have used to calculate the expected X-ray emission from the shocked shell of gas as a function of the ambient gas density for 1345+125 and 2352+495 (Fig. 4). These calculations assume a low efficiency of conversion[6] of jet power into radio power (a value of Bicknell et al.'s $\kappa = 10^{-12}$ or alternately $\epsilon \simeq 4\%$), which gives jet powers of order a few times 10^{45} ergs s^{-1}. For expected ambient densities of order 0.1–1 cm^{-3}, the predicted X-ray luminosity is less than (for 1345+125) or of order (for 2352+495) 10^{41} ergs s^{-1} and is 2 orders of magnitude below the sensitivity of our current observations. Thus, our current observations are consistent with the Heinz et al. model, although deeper observations are needed for a strong test of the model.

3.3. *Constraints on the Ionization of the Optical Emission Lines*

Is the emission-line luminosity of these sources consistent with photoionization by the AGN continuum estimated from our X-ray observations? The number of ionizing photons required to power the nebula is given by

$$Q_{\mathrm{tot}} = \frac{2.2 L_{\mathrm{H}\alpha}}{h\nu_{\alpha}}, \quad (1)$$

[5] We have compared our results to those of BLRGs since to our knowledge no powerful narrow line radio galaxies have yet been detected by *ASCA*.

[6] If the efficiency is higher than we have assumed, the derived jet power would be lower and the predicted X-ray luminosity of the shocked gas would also be lower.

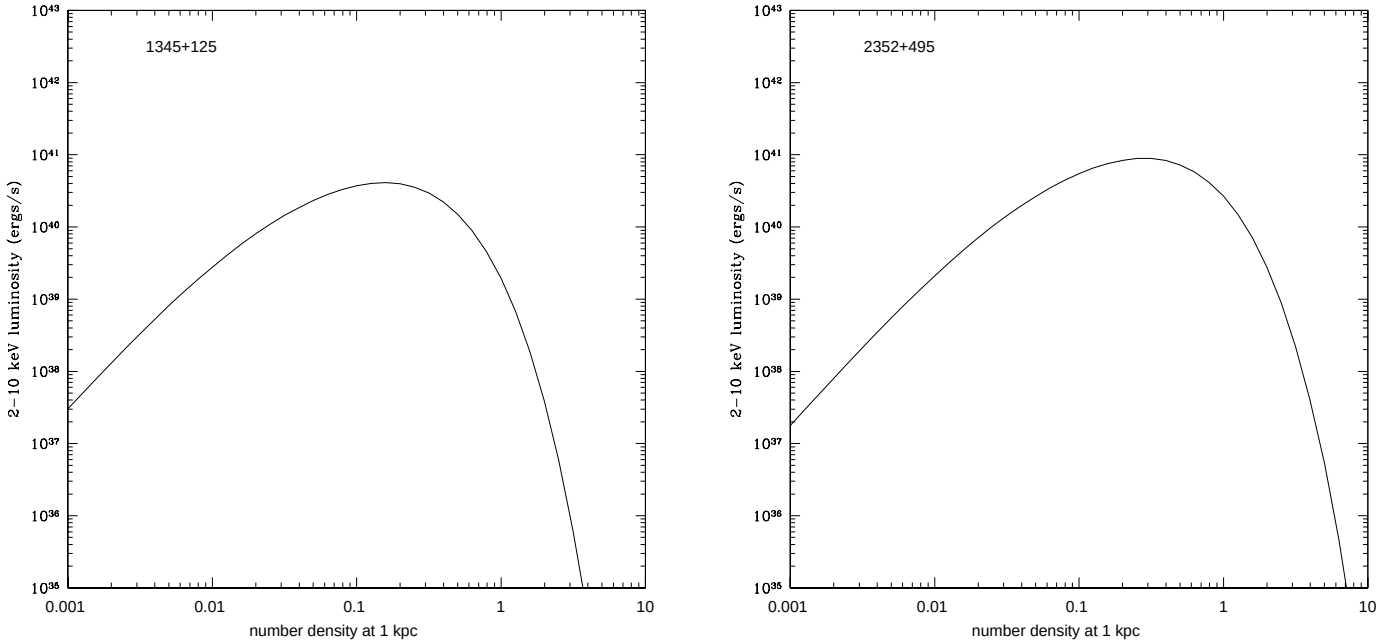


FIG. 4.—Expected bremsstrahlung X-ray luminosity in the 2–10 keV band from a shocked shell of gas around the expanding radio source (see Heinz et al. 1998). The X-ray luminosity is plotted as a function of the ambient density at 1 kpc. Curves are calculated using a program obtained courtesy of Chris Reynolds. *Left*: 1345+125. *Right*: 2352+495.

where $L_{\mathrm{H}\alpha}$ and ν_α are the luminosity and frequency of the Hα line and h is Planck's constant and case B recombination is assumed (e.g., Baum & Heckman 1989).

The number of ionizing photons in the spectral region above 13.6 eV is partially constrained by our ROSAT and *ASCA* observations, but depends on an uncertain extrapolation to 13.6 eV since we do not know the shape of the continuum. For a power-law spectrum, the number of ionizing photons produced by the nucleus is

$$Q_{\mathrm{nuc}} = 4\pi D_{\mathrm{lum}}^2 \int_{\nu_1}^{\nu_2} \frac{S_0\, \nu^{-\alpha}}{h\nu}\, d\nu\ , \qquad (2)$$

where D_{lum} is the luminosity distance, the flux density at frequency ν is given by $S_\nu = S_0 \nu^{-\alpha}$, ν_1 is the lower frequency cutoff (13.6 eV = 3.26×10^{15} Hz), and ν_2 is the upper frequency cutoff[7] (e.g., Baum & Heckman 1989; Wilson, Ward, & Haniff 1988).

For example, in 2352+495, $L_{\mathrm{H}\alpha} \simeq 1 \times 10^{41}$ ergs s^{-1} (Lawrence et al. 1996), giving a required flux of $Q_{\mathrm{tot}} \simeq 7.4 \times 10^{52}$ photons s^{-1}, which is comparable to other radio galaxies in the Baum & Heckman (1989) sample. We adopt $S_\nu < 1.8 \times 10^{-2}$ μJy at 1 keV for 2352+495. For $\alpha = 1$ (the slope used by Baum & Heckman 1989) we obtain $Q_{\mathrm{nuc}} < 2 \times 10^{51}$ photons s^{-1}, which is not enough to power the emission lines.

Our results for 1345+125 and 2352+495 are given in Table 7 and plotted in Figure 5. Here we have adopted $\alpha = 1$; note that changing α by 0.5 changes Q_{nuc} by a factor about 5, in the sense that for a given X-ray flux a steeper spectral index results in more ionizing photons. For comparison, we plot the powerful extended radio galaxies from Baum & Heckman and the Seyfert 1's from Reynolds (1997). The powerful radio galaxies and the Seyfert 1's are in agreement and are consistent with the AGN producing sufficient

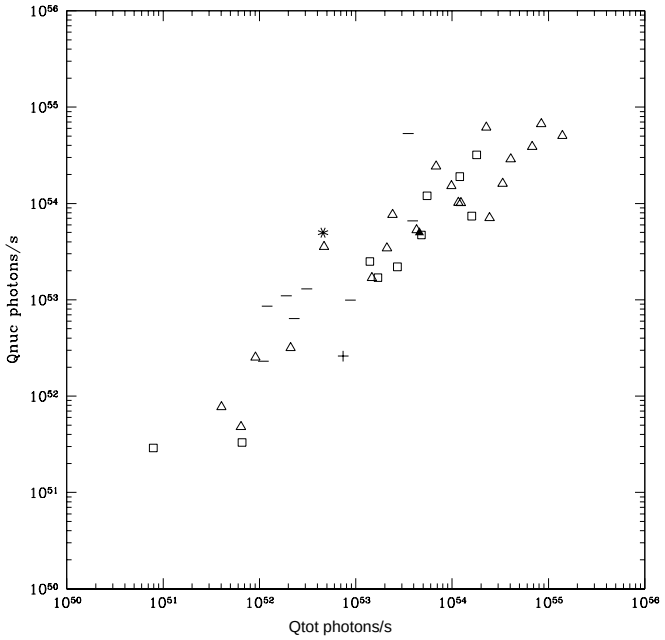


FIG. 5.—Ionizing photon rate produced by the nucleus (Q_{nuc}) vs. the photon rate required to produce the emission-line luminosity (Q_{tot}). We adopt $\alpha = 1$ for the slope of the ionizing continuum. The squares and horizontal lines are estimates and upper limits, respectively, from Table 6 of Baum & Heckman (1989). The plus sign is the upper limit on Q_{nuc} for 2352+495. The filled triangle shows the X-ray derived Q_{nuc} for 1345+125 plotted vs. the Q_{tot} derived from the observed emission-line luminosity of the western active nucleus, while the asterisk indicates the upper limit on Q_{tot} for the nonactive eastern nucleus derived from the upper limit to the emission-line luminosity. The open triangles are Seyfert 1 galaxies from the *ASCA* study of Reynolds (1997), and the emission-line fluxes used to estimate Q_{tot} are taken from the literature (mostly from Whittle 1992). The Reynolds Seyfert 1's and the Baum and Heckman radio galaxies are in good agreement and are consistent with the emission-line gas being photoionized by the AGN continuum.

[7] For the slopes we use, the upper frequency cutoff is not important.

TABLE 7

CONSTRAINTS ON IONIZING PHOTONS

Source	Q_{nuc} (photons s^{-1})	Q_{tot} (photons s^{-1})
1345+125 (active nucleus)	5.0×10^{53}	4.6×10^{53}
1345+125 (nonactive nucleus).....	5.0×10^{53}	$<4.6 \times 10^{52}$
2352+495.....	$<2.6 \times 10^{52}$	7.4×10^{52}

NOTE.—Q_{nuc} is the number of ionizing photons produced by the AGN estimated from our X-ray observations and assuming a spectrum with a power-law slope of $\alpha = 1$. Q_{tot} is the number of ionizing photons required to produced the observed emission-line luminosity (1345+125, Baum & Heckman 1989; 2352+495, Lawrence et al. 1996).

TABLE 8

X-RAY PROPERTIES OF SHOCKS

Shock Velocity (km s^{-1})	X-ray Color [log(0.2–2/2–10)]	L(2–10 keV) (ergs s^{-1})
300	10.0	5.2E29
400	5.85	4.0E34
500	3.97	9.7E36
600	3.00	1.5E38
700	2.33	9.3E38
800	1.90	4.9E39
850	1.74	7.7E39
900	1.59	1.1E40

ionizing photons to power the emission-line luminosity. We calculate Q_{tot} separately for both the nonactive eastern nucleus and the GPS western nucleus in 1345+125. In 1345+125, the emission-line luminosity of the western nucleus is consistent with photoionization by the detected X-rays. This is consistent with the X-ray emission also being produced by the western nucleus. On the other hand, the nonactive nucleus of 1345+125 would be "underluminous" in emission lines if it were the source of the X-ray emission.

In contrast, the emission lines in 2352+495 seem somewhat over-luminous, given our upper limit on the X-ray luminosity. This needs to be confirmed by deeper observations. It is possible that the emission lines are ionized by AGN photons which are obscured from our view (see e.g., Axon et al. 1999). Alternately, such a deficit in nuclear ionizing photons would be consistent with a scenario where at least some of the emission-line luminosity is powered by shocks produced by interaction of the gas with the radio source. This interaction has been suggested for GPS and CSS sources (Bicknell, Dopita, & O'Dea 1997; Begelman 1998) and is supported by the existence of emission-line gas aligned with some CSS radio sources (De Vries et al. 1997, 1999; Axon et al. 1999).

In Table 8 we tabulate the X-ray luminosity expected if the observed line emission were entirely produced by shocks with fully ionized precursors. We have calculated X-ray emission in the 2–10 keV energy band for a range of shock velocities using the MAPPINGS II shock code (Dopita & Sutherland 1995, 1996). The X-ray emission from the post-shock material is relatively soft, as demonstrated by the ratio of 0.2–2/2–10 keV emission, and significant amounts of X-ray emission above 1 keV are only produced by shocks with velocities above about 600–700 km s^{-1}. The energy distribution of X-rays produced simply corresponds to the temperature of the post-shock gas. Even for the highest shock velocities that we have calculated, the 2–10 keV X-ray emission is still significantly below our *ASCA* detection limit.

4. CONCLUDING REMARKS

Thus, our *ASCA* observations have only deepened the mystery of the GPS sources. More sensitive observations will be needed (1) to determine whether the GPS galaxies have low AGN luminosities and low absorbing columns or high AGN luminosities and high absorbing columns, and (2) to determine whether there are sufficient ionizing photons produced by the nucleus to power the observed narrow emission-line luminosity, (3) to test the evolving source model of Heinz et al. (1998), and (4) to compare the extended gaseous environments with those of what are believed to be the more highly evolved counterparts of GPS sources.

We are grateful to Chris Reynolds for providing the code used to calculate the model curves in Figure 4 and for comments on the manuscript, and to Carlo Stanghellini, Bruce Woodgate, and Aaron Evans for helpful discussions. C. P. O. and S. A. B. are grateful to Carnegie Observatories and Princeton University for their hospitality during which most of this paper was written. This research was partially supported by NASA grant NAG 5-3405 from the *ASCA* Guest Observer Program. W. D. V. was partially supported by the STScI Director's Discretionary Research Fund. This research made use of (1) the NASA/IPAC Extragalactic Database (NED) which is operated by the Jet Propulsion Laboratory, California Institute of Technology, under contract with the National Aeronautics and Space Administration, and (2) NASA's Astrophysics Data System Abstract Service.

REFERENCES

Allen, S. W., Fabian, A. C., Idesawa, E., Inoue, H., Kii, T., & Otani, C. 1997, MNRAS, 286, 765
Axon, D. J., Capetti, A., Fanti, R., Morganti, R., Robinson, A., & Spencer, R. 1999, MNRAS, submitted
Baum, S. A., & Heckman, T. M. 1989, ApJ, 336, 681
Baum, S. A., Heckman, T., Bridle, A., van Breugel, W., & Miley, G. 1988, ApJS, 68, 643
Baum, S. A., Heckman, T., & van Breugel, W. 1992, ApJ, 389, 208
Begelman, M. C. 1996, in Cygnus A: Study of a Radio Galaxy, ed. C. Carilli & D. Harris (Cambridge: Cambridge Univ. Press), 209
———. 1998, in The Most Distant Radio Galaxies, ed. H. J. A. Röttgering, P. Best, & M. D. Lehnert (Dordrecht: Kluwer), 173
Bicknell, G., Dopita, M. A., & O'Dea, C. P. 1997, ApJ, 485, 112
Bloemen, J. B. G. M., et al. 1986, A&A, 154, 25
Brunetti, G., Comastri, A., Setti, G., & Feretti, L. 1999, A&A, 342, 57
Carvalho, J. C. 1985, MNRAS, 215, 463
Conway, J. E. 2000, in Lifecycles of Radio Galaxies, ed. J. A. Biretta, A. M. Koekemoer, C. P. O'Dea, & E. Perlman (Amsterdam: New Astron. Rev.), in press
de Vries, W. H., et al. 1997, ApJS, 110, 191
de Vries, W. H., O'Dea, C. P., Baum, S. A., & Barthel, P. D. 1999, ApJ, 526, 27
De Young, D. S. 1997, ApJ, 490, L55
Dopita, M. A., & Sutherland, R. S. 1995, ApJ, 455, 468
———. 1996, ApJS, 102, 161
Evans, A. S., Kim, D. C., Mazzarella, Scoville, N. Z., & Sanders, D. B. 1999, ApJ, 521, L107
Fanti, R., Fanti, C., Schilizzi, R. T., Spencer, R. E., Rendong, N., Parma, P., van Breugel, W. J. M., & Venturi, T. 1990, A&A, 231, 333

Fanti, C., Fanti, R., Dallacasa, D., Schilizzi, R. T., Spencer, R. E., & Stanghellini, C. 1995, A&A, 302, 317
Gallimore, J., Baum, S. A., O'Dea, C. P., Pedlar, A., & Brinks, E. 1999, ApJ, 524, 684
Gelderman, R., & Whittle, M. 1994, ApJS, 91, 491
Gilmore, G., & Shaw, M. A. 1986, Nature, 321, 750
Golombek, D., Miley, G. K., & Neugebauer, G. 1988, AJ, 95, 26
Grandi, S. A. 1977, ApJ, 215, 446
Heinz, S., Reynolds, C. S., & Begelman, M. C. 1998, ApJ, 501, 126
Heckman, T. M., Smith, E. P., Baum, S. A., van Breugel, W. J. M., Miley, G. K., Illingworth, G. D., Bothun, G. D., & Balick, B. 1986, ApJ, 311, 526
Hurt, T., Antonucci, R., Cohen, R., Kinney, A., & Krolik, J. 1999, ApJ, 514, 579
Hutchings, J. B. 1987, ApJ, 320, 122
Kim, D.-C., Veilleux, S., & Sanders, D. B. 1998, ApJ, 508, 627
Kriss, G. A., Canizares, C. R., & Ricker, G. R. 1980, ApJ, 242, 492
Lawrence, C. R., Zucker, J. R., Readhead, A. C. S., Unwin, S. C., Pearson, T. J., & Xu, W. 1996, ApJS, 107, 541
Maloney, P. R., Begelman, M. C., & Rees, M. J. 1994, ApJ, 432, 606
Mirabel, I. F. 1989, ApJ, 340, L13
Mirabel, I. F., Sanders, D. B., & Kazes, I. 1989, ApJ, 340, L9
Nandra, K., George, I. M., Mushotzky, R. F., Turner, T. J., & Yaqoob, T. 1997, ApJ, 476, 70
O'Dea, C. P. 1998, PASP, 110, 493
O'Dea, C. P., & Baum, S. A. 1997, AJ, 113, 148
O'Dea, C. P., Baum, S. A., & Stanghellini, C. 1991, ApJ, 380, 66
O'Dea, C. P., Stanghellini, C., Baum, S. A., & Charlot, S. 1996a, ApJ, 470, 806
O'Dea, C. P., Worrall, D. M., Baum, S. A., & Stanghellini, C. 1996b, AJ, 111, 92 (Paper I)
Owsianik, I., & Conway, J. E. 1998, A&A, 337, 69
Readhead, A. C. S., Taylor, G. B., Pearson, T. J., & Wilkinson, P. N. 1996a, ApJ, 460, 634
Readhead, A. C. S., Taylor, G. B., Xu, W., Pearson, T. J., Wilkinson, P. N., & Polatidis, A. G. 1996b, ApJ, 460, 612
Reeves, J. N., Turner, M. J. L., Ohashi, T., & Kii, T. 1997, MNRAS, 292, 468
Reynolds, C. S. 1997, MNRAS, 286, 513
Sambruna, R. M., George, I. M., Mushotzky, R. F., Nandra, K., & Turner, T. J. 1998, ApJ, 495, 749
Sanders, D. B., Soifer, B. T., Elias, J. H., Neugebauer, G., & Matthews, K. 1988, ApJ, 328, L35
Scoville, N. Z., & Sanders, D. B. 1987, in Interstellar Processes, ed. D. Hollenbach & H. Thronson (Dordrecht: Reidel), 21
Snellen, I. A. G., Schilizzi, R. T., de Bruyn, A. G., & Miley, G. K. 1998, A&A, 333, 70
Stanghellini, C., O'Dea, C. P., Baum, S. A., Dallacasa, D., Fanti, R., & Fanti, C. 1997, A&A, 325, 943
Stanghellini, C., O'Dea, C. P., Baum, S. A., & Laurikainen, E. 1993, ApJS, 88, 1
Surace, J. A., Sanders, D. B., Vacca, W. D., Veilleux, S., & Mazzarella, J. M. 1998, ApJ, 492, 116
Turner, T. J., George, I. M., Nandra, K., & Mushotzky, R. F. 1998, ApJ, 493, 91
———. 1997, ApJS, 113, 23
Veilleux, S., Sanders, D. B., & Kim, D.-C. 1997, ApJ, 484, 92
Whittle, M. 1992, ApJS, 79, 49
Wilson, A. S., Ward, M. J., & Haniff, C. A. 1988, ApJ, 334, 121
Woźniak, P. R., Zdziarski, A. A., Smith, D., Madejski, G. M., & Johnson, W. N. 1998, MNRAS, 299, 449
Young, J. S., & Scoville, N. Z. 1991, ARA&A, 29, 581